17th Brazilian Congress of Thermal Sciences and Engineering
November 25th-28th, 2018, Águas de Lindóia, SP, Brazil

ENCIT-2018-0497
BOILING HEAT TRANSFER BEHAVIOR FOR NANOCOATED SURFACES UNDER CONFINED CONDITIONS

Jéssica Martha Nunes[1]
jessicamn.engmec@gmail.com
Reinaldo Rodrigues de Souza[1]
reisartre@gmail.com
Elaine Maria Cardoso[1]
elaine.cardoso@unesp.br
[1]UNESP – São Paulo State University, Post-Graduation Program in Mechanical Engineering, Av. Brasil Centro, 56, 15385-000 Ilha Solteira, SP, Brazil

Abstract. *Nanocoating techniques have been used to increase the heat transfer coefficient by changing the surface morphology, which could potentially increase the heat transfer in case of pool boiling systems. The present work aims to study the effect of nanocoated surfaces and the gap size during the pool boiling of deionized water, at atmospheric pressure and saturation temperature. The tests were performed on copper heating surfaces with two different roughness values, corresponding to smooth and rough surfaces. The nanocoated surfaces were produced by alumina (Al_2O_3) nanoparticle deposition with 0.3 g/l volumetric concentration, via nanofluid boiling process. A gap size of 1.0 mm, corresponding to Bond number equal to 0.4, was analyzed in this study. Concerning to the heat transfer coefficient, the coated surfaces showed deteriorations in the HTC as compared with the uncoated ones mainly due to the fouling resistance formed on the heating surface, confirmed by the surface characterization (SEM images). The coating process significantly increases the surface wettability, which in turn, increases the re-wetting capacity during the confined boiling process. It was observed an enhancement of 52% in the dryout heat flux, for smooth surfaces with coating layer.*

Keywords: *Boiling heat transfer, nanocoated surface, confined nucleate boiling.*

1. INTRODUCTION

Technological advances in electronic devices packing high processing capacity in reduced size imply the adoption of more efficient heat transfer methods. New techniques to improve the heat transfer coefficient (HTC) and the critical heat flux (CHF) have been researched. One of them is the boiling process, which is widespread in the scientific community due to its high heat removal capacity.

Since the pioneer work of Ishibashi and Nishikawa (1969) about confined nucleate boiling up to recent studies related to confined boiling and modified surfaces (Yang and Liu, 2013, Souza et al., 2014, Souza et al., 2018), the nucleate boiling regime is one of the most important heat transfer mechanism. The gap size effect can be characterized by a dimensionless number known as the Bond number, *Bo*, defined as the ratio of the characteristic length to the confined space, *s*, and the capillary length, *L*, proportional to the detachment diameter of the vapor bubble (Yao and Chang, 1983). Thus, the heat transfer coefficient (HTC) can also be modified by the confinement of the system using, for example, an unheated surface.

The characteristic most commonly observed in the confined nucleate boiling regime as compared with an unconfined case is the heat transfer enhancement for low and moderated heat fluxes values and the degradation for high heat fluxes (Katto et al. 1977, Passos et al. 2004, Cardoso et al. 2011, Cardoso and Passos, 2013). According to Ishibashi and Nishikawa (1969) and Katto et al. (1977), this behavior can be due to evaporation of a liquid film present between the flattened vapor bubble and the heating surface, which in turn, increases the boiling heat transfer.

Nowadays, coating techniques have been used to increase the HTC or critical heat flux (CHF) by changing the heating surface morphology. Yang and Liu (2013) pointed out three different causes to explain how the heat transfer coefficient is affected by surfaces with microporous coatings: (i) number of active nucleation sites; (ii) bubble residence time on the heating surface; and, (iii) thermal resistance of the microporous coating layer. For confined nucleate boiling, the unheated surface can hinder the vapor from leaving the heating surface, leading to an increase in the wall superheating and, consequently, a decrease in the heat transfer performance.

Souza et al. (2014) studied the influence of nanoparticle size and gap size on pool boiling. Those authors used different nanoparticles diameters (10 nm and 80 nm), different gap sizes, and as the working fluid, HFE7100 at saturated conditions. For coated rough surfaces - R_a = 0.16 µm and nanoparticles of 10 nm diameter - and gap size of 0.1 mm, an increase in the HTC of around 145% was observed for heat fluxes lower than 45 kW/m^2; for coated rough

surfaces with nanoparticles of 80 nm, the results showed a decrease in the boiling heat transfer.

Moreover, Souza et al. (2018) presented the results for confined boiling on a smooth heating surface (R_a = 0.02 μm). The HTC increased by 100% for heat flux values close to 40 kW/m^2 and for surfaces with deposition of maghemite nanoparticles of 80 nm diameter. However, for heat flux values higher than 40 kW/m^2, it was observed a decrease in the HTC. For coated surfaces, the confinement led to an enhancement in the boiling heat transfer regardless of the nanoparticle size; however, for uncoated ones, it was observed HTC degradation of around 21%.

The above bibliographic review shows that only a few studies are available for confined nucleate boiling on nanocoated surfaces. In this context, the present work aims to analyze how the coated surfaces influence the boiling heat transfer behavior of DI-water under confined conditions. By using DI-water as working fluid, the heating surface-fluid interaction such as, surface roughness and wettability, can be evaluated.

2. MATERIALS AND METHOD

2.1 Test surfaces preparation

Table 1 shows the experimental conditions tested in this study. The uncoated heating surfaces consisted of one smooth surface (namely, SS) and one rough surface (namely, RS). The coated surfaces were produced by the boiling process of Al_2O_3-deionized water nanofluid with 0.3 g/l mass concentration. The gap size of s = 1.0 mm, corresponding to the Bo = 0.4, was analyzed in the present study.

The rough surfaces were polished with #400 emery paper, corresponding to an average surface roughness (R_a) of 0.33 μm. The smooth surfaces were mechanically polished with aluminum-oxide compound, resulting in an average surface roughness of 0.05 μm. After the polishing process, in order to clean the surfaces, they were put into an ultrasonic bath during 5 minutes and cleaned with acetone.

Table 1. Description of the experimental conditions tested in the present study.

Heating surface	Surface condition	Gap size, s (mm)
Smooth surface (polished with aluminum-oxide abrasive compound)	Uncoated	1.0 (SS)
	Coated*	1.0 (SS-Nano)
Rough surface (polished with #400 emery paper)	Uncoated	1.0 (RS)
	Coated*	1.0 (RS-Nano)

*by nanofluid boiling process with 0.3 g/l mass concentration.

The alumina nanofluid was prepared by the 2-step method, consisting in direct mixing of alumina powder nanoparticles (10 nm average diameter) in DI-water at the desired mass concentration followed by ultrasonic agitation for 3 hours to avoid clusters formation.

2.2 Apparatus assembly

A test section, two thermostatic baths, an electrical power source, a data acquisition Agilent 34970A model, and a computer composed the experimental setup, as shown in Fig. 1.

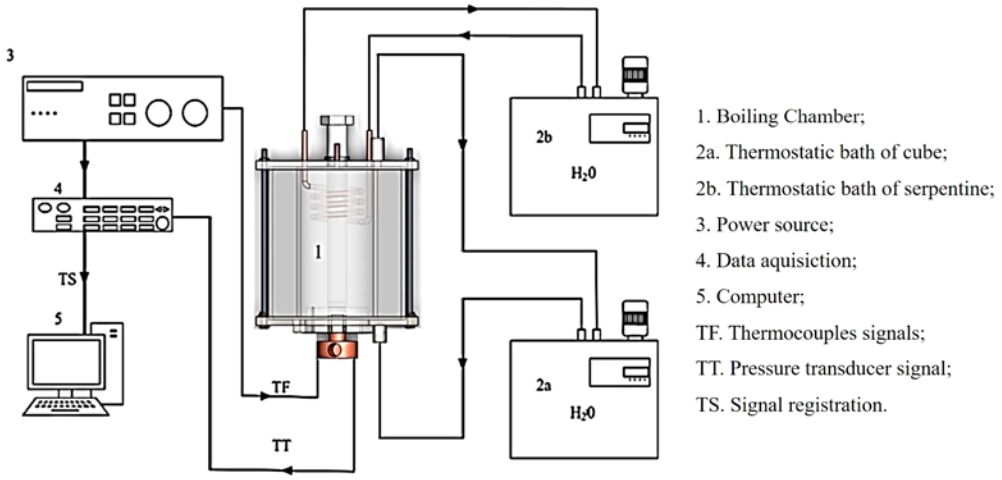

Figure 1. Schematic drawing of the experimental apparatus.

The boiling chamber (Fig. 2) consisted of a cube vessel of 5 mm thick glass walls and overall dimensions 170 x 170 x 180 mm, that involves a borosilicate tube of 90 mm internal diameter, 180 mm height, and 6 mm wall thickness. The cube vessel and the tube are fixed between two plates of stainless steel (AISI 316). Inside the tube, there is a condenser made by a copper serpentine and the element for confinement. The confinement of the boiling space is set by a PVC element (250 mm in length and 20 mm in diameter), mounted on the end of a stainless steel tube.

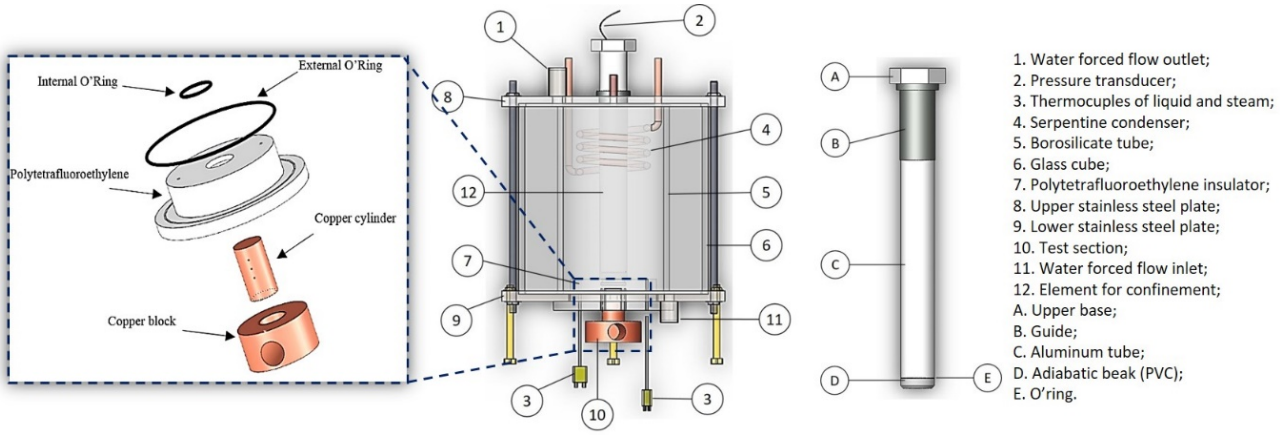

Figure 2. Boiling chamber and details of the confined element, including the test section.

In the space between the vessel and the tube there was a forced flow of water whose temperature was controlled by a thermostatic bath, in order to maintain the temperature of the working fluid near the saturation temperature (at atmospheric pressure, T_{sat} = 99 °C). A second thermostatic bath controls the temperature of the condenser located at the top of the boiling chamber to minimize evaporation losses.

The test section consisted of a copper block (20 mm diameter) with three K-type thermocouples, fixed in the cylindrical part to determine the wall temperatures and the heat flux. The copper block is heated by one cartridge resistance with a maximum power of 300 W. The thermal insulation of the test section consists of polytetrafluoroethylene and vermiculite.

2.3 Experimental Procedure

The experiments were conducted using deionized water (DI-water) as the working fluid under saturated conditions at a pressure close to 98 kPa. Before each run, the working fluid was heated very close to the saturation temperature in order to degas it. No evidence of significant amounts of gas dissolved in the working fluid was detected on the boiling curves. Before each series of measurements, vacuum was created in the boiling chamber and, then, this vessel was immediately fed with the working fluid. The test conditions were regulated by monitoring the pressure and the temperature inside the boiling chamber. The same procedure was adopted during all the experimental tests in order to ensure repeatability.

When the apparatus reaches the saturation temperature in a steady state, heat fluxes in a range of 100 kW/m² to CHF (*Critical Heat Flux*) were applied increasing in steps of 70 kW/m². The CHF was characterized by the non-stability of heating surface temperature.

The heat flux and surface temperature were calculated according to Fourier's Law assuming 1-D conduction based on the wall temperature measurements from the thermocouples embedded in the copper block. The temperature of the boiling surface was then determined by extrapolating the linear temperature profile to the copper block upper surface, T_w. The setup of the block and the location of the thermocouples are shown in Fig. 3.

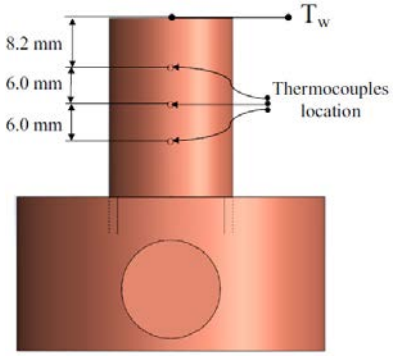

Figure 3. Copper heating surface.

Finally, the heat transfer coefficient was calculated using Newton's law of cooling given by:

$$h = \frac{q''}{\Delta T_{sat}} \tag{1}$$

where $\Delta T_{sat} = T_w - T_{sat}(p_{atm})$. T_w is the wall temperature, and $T_{sat}(p_{atm})$ corresponds to the saturation temperature of water at local atmospheric pressure (p_{atm} = 98 kPa).

The distance between the heating surface and the confined element was adjustable by turning the stainless tube and was controlled by a dial. The acquisition of the signals from the thermocouples and the voltage applied to the resistance, as well as the pre-treatment of the data, were carried out with an Agilent 34970A system.

The temperature uncertainty was ± 0.4 ºC. For all surfaces tested, the experimental uncertainty for the heat flux and heat transfer coefficient varied from 1.7% to 14.3% and from 2.3% to 15.1%, respectively. A comparison between the imposed heat flux based on the current and voltage measurements, and the heat flux estimated from the linear profile revealed heat losses always lower than 15%. The experimental procedure was the same to that described by Nunes et al. (2017).

2.4 Wettability measurement

Figure 4 presents the experimental apparatus used to capture images of the sessile drops before being analyzed for static contact angles. It consists of a test surface, a camera, a green LED light source, a light diffuser and an aluminum plate where the test surface is fixed.

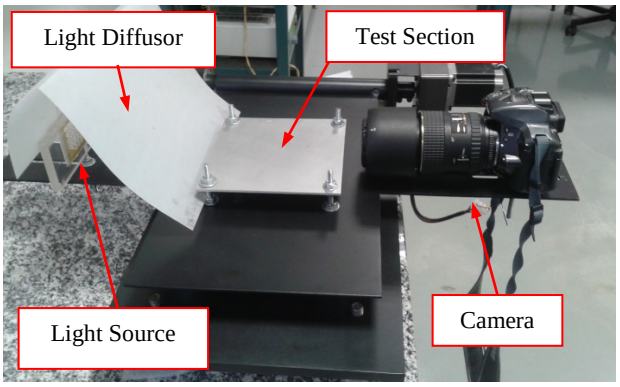

Figure 4. Experimental setup used to capture the sessile drops images.

The procedure adopted to evaluate the static contact angle consists of depositing on the test surface a sessile droplet of DI-water with a volume of 10 µl through a micropipette pointed vertically down onto the sample. Then, a camera captures the images of the droplet on the surface. After that, the pictures are analyzed using image post-processing software to shape the deionized water droplet. The adopted procedure is well detailed by Kiyomura et al. (2017).

3. RESULTS AND DISCUSSION

The results for the roughness measurements, R_a (µm), static contact angle (wettability) and SEM images of the samples before the boiling tests under confined conditions are presented in Table 2. The coating process leads to an increase in surface roughness as compared to the uncoated ones, regardless the original heating surface condition. This augmentation in the surface roughness also reflects in a wettability enhancement, characterized by a drastic decrease in the static contact angle.

The images for wettability in Tab. 2 depict surface-fluid interaction conditions of sessile droplets of DI-water (with a volume of 10 µl) onto the smooth and rough surfaces before and after coating process. According to the results displayed, the heating surface wettability and the static contact angle are functions of the original surface condition and coating process. These results agree with Takata et al. (2005) who reported that surface wettability is inversely proportional to contact angle.

Table 2. Average surface roughness, static contact angle and SEM images for all surfaces tested.

	SS	SS-Nano	RS	RS-Nano
Surface roughness, R_a (μm)	0.05	0.52	0.33	0.55
Static contact angle, θ (°)	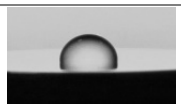 91°	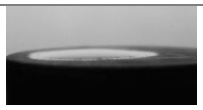 < 10°	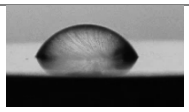 68°	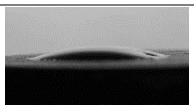 16°
SEM images (before the boiling tests under confined conditions)	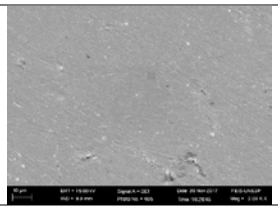	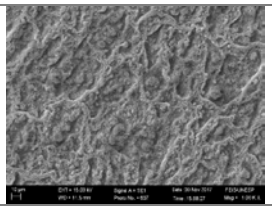	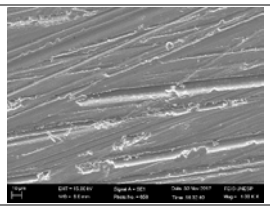	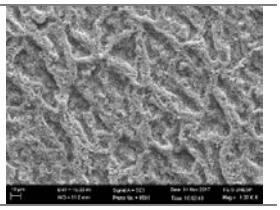

Figures 5a and 5b shows the HTC curves under confined conditions for the smooth and rough surfaces, respectively. HTC degradation is observed for coated surfaces as compared to the uncoated ones, and this behavior can be explained by the nanolayer formed on the heating surface that increases the thermal resistance, degrading the HTC.

The smooth uncoated surface (Fig. 5a) presents lower nucleation sites density due to the lower roughness. Thus, the coating process - which increases the surface roughness and, consequently, the density of the nucleation sites - may positively affect HTC behavior. Nevertheless, this effect is counterbalance with the increase of the thermal resistance formed by the nanolayer, resulting in an average decrease of 11% in the HTC for SS-Nano.

For rough uncoated surface (Fig. 5b), where the original surface roughness contributes to the heat transfer, the nanocoating causes a clogging effect of the pre-existing cavities on the surface, degrading HTC; moreover, the thermal resistance formation due to coating layer, leads to a degradation of around 29% in HTC for RS-Nano.

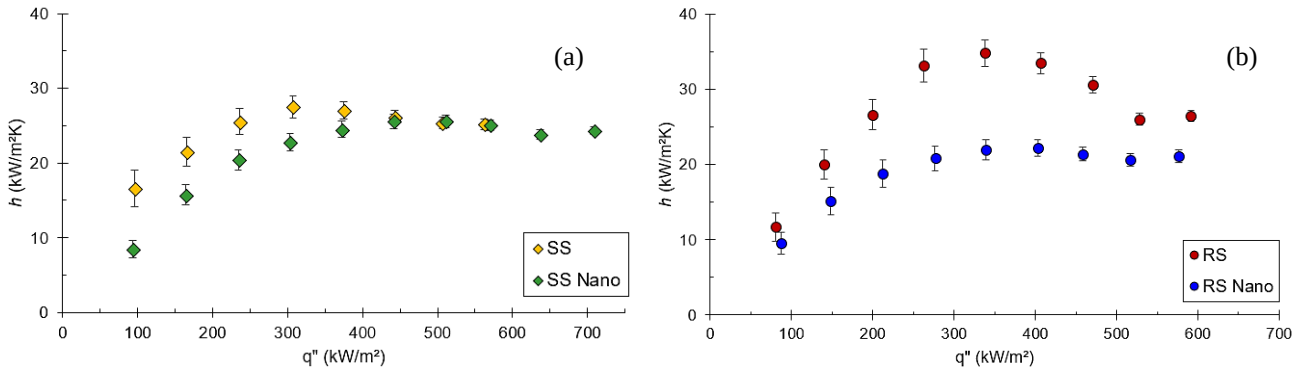

Figure 5. HTC curves under confined conditions for uncoated and coated surfaces. (a) smooth surfaces and (b) rough surfaces.

For low and moderated heat fluxes ($q" \leq 350$ kW/m^2), the confined condition promotes an intensification of the boiling heat transfer; the vapor bubble deformation and the increase in the residence time of the bubbles on the heating surface promotes the liquid film evaporation located between the heating surface and the vapor bubble, leading to a HTC enhancement. As the heat flux increases, the vapor bubble frequency also increases creating a large mass of vapor in the gap that inhibits the cooling effect of the heating surface, degrading the HTC.

Figure 6 shows the images taken during the test with uncoated rough surface (RS), at low heat flux (100 kW/m²) and at moderated heat fluxes (660 kW/m², corresponding to the heat flux close to the CHF). One may observe that, at low heat flux value (Fig. 6a) the bubbles are small and there is no vapor trapped between the surface and the confined element. Instead, at moderated heat flux value (Fig. 6b), it is noticeable the coalescence of vapor bubbles that stay trapped between the surface and the confined element.

The coating process leads to a dryout delay in the confined tests, which can be explained by the fact that the nanostructures influence the surface/fluid interaction mechanisms, increasing the surface wettability, which is a pronounced effect for non-wetting fluids, as the DI-water. As the surface wettability increases the re-wetting process also increases, improving the surface cooling. For confined conditions, the vapor mass trapped in the gap inhibits the re-wetting process and, the uncoated surfaces (RS and SS) reach the dryout earlier as compared to the coated surfaces.

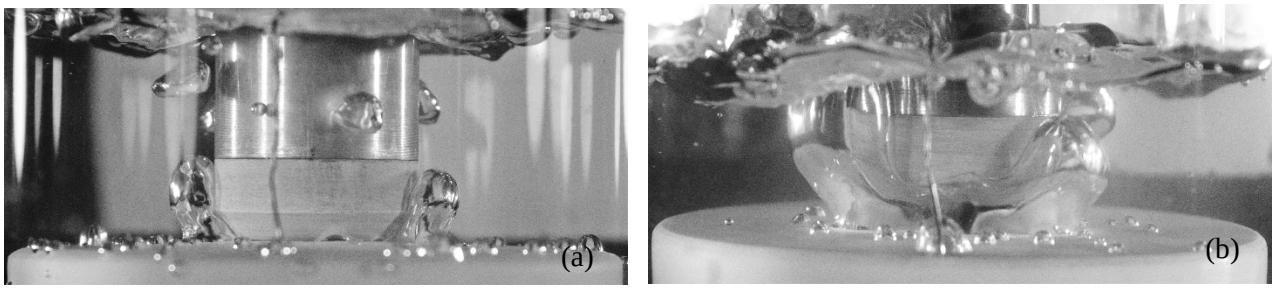

Figure 6. RS test images for low and moderated heat flux applied. a) for 100 kW/m² and b) for 660 kW/m², respectively.

It was possible to determine the dryout heat flux by fitting the HTC curves with a polynomial curve, where the dryout incipience is represented by the maximum point of the parabolic region in the HTC curves adjusted. For the SS-Nano, the dryout occurred at 470 kW/m², increasing 52% compared with the SS; and, for the RS-Nano, the dryout occurred at 411 kW/m², increasing 28% compared with the RS surface.

Figure 7 shows the SEM images for the nanocoated surfaces, SS-Nano and RS-Nano, after the DI-water boiling tests. These images show that changes in the surface morphology occurred due to the effects of the confinement. Some regions present characteristics of sintering, where the outer nanocoating layer shows a more homogeneous and smoother appearance; the inner layers show a different characteristic, with porous layers and clusters formation.

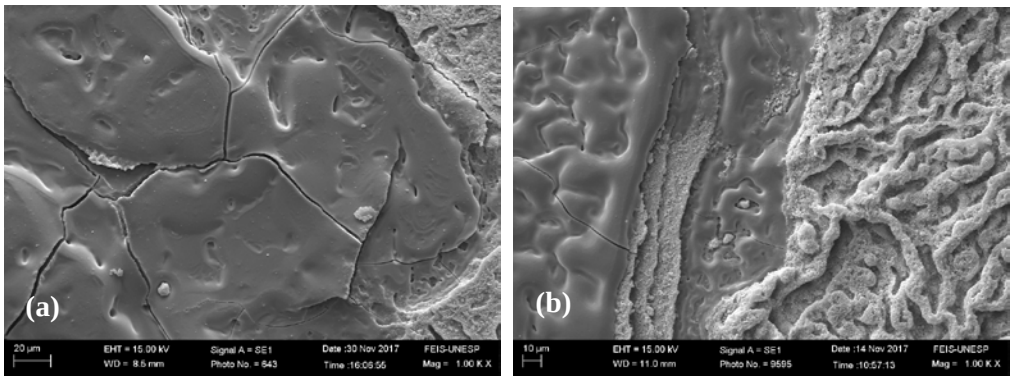

Figure 7. SEM images of the nanocoated regions showing changes in the surface morphology after the confined boiling tests. (a) SS-Nano and (b) RS-Nano.

The images presented in Fig. 7 require further studies including Raman and Energy Dispersive Spectroscopy (EDS) analyses on the original and nanocoated surfaces to verify possible structural differences, since the process of changing the surface morphology may involve more than one physical mechanism.

One possible explanation for the change in the surface morphology, after the boiling tests, could be the vapor bubble dynamic and the increase in the residence time of the vapor bubble on the heating surface under confined conditions; the vapor mass trapped in the channel puts pressure on the nanocoated layer, deforming the original structure of the nanolayer. Similar characteristics are found in the powder metallurgy process, where high pressure is applied to squeeze the powder into the desired shape and heat, below the melting point, allows solid-state diffusion and bond the particles together.

4. CONCLUSION

We analyze the effect of heating surface roughness and coating process on the boiling heat transfer, under confined conditions, using DI-water as the working fluid. After coating the heating surface by using nanofluid pool boiling process, we perform the wettability and surface roughness characterization. The main results are summarized as follows:

- ✓ The coating layer formed on the heating surface by the nanofluid pool boiling process increases the surface wettability, characterized by the decrease in the static contact angle;
- ✓ The coating layer formed on the heating surfaces provides a barrier to the heat transfer increasing the thermal resistance of the surface, therefore degrading the HTC, for both smooth and rough surfaces under confined conditions;

- ✓ The confinement enhances the HTC for low and moderated heat fluxes, because the vapor bubbles coalescence and stay longer on the heating surface, promoting the evaporation of the liquid film located between the heated surface and the vapor bubble. As the heat flux increases, a mass of vapor is trapped on the heating surface, anticipating the dryout phenomenon and, consequently, reaching the CHF early.
- ✓ The coating process delays the dryout occurrence under confined conditions due to the influence of the nanostructures on the surface/fluid interaction mechanisms such as, the surface wettability, which is a pronounced effect for non-wetting fluids, as the DI-water.
- ✓ The hypothesis of solid-state diffusion of the nanoparticles caused by the mechanical squeeze of the vapor bubbles in the confined region, similar to that found in the powder metallurgy process, was used to explain the images. However, this hypothesis requires further studies including Raman and Energy Dispersive Spectroscopy (EDS) analyses to verify possible structural differences between the original and coated surfaces, since the process of changing the surface morphology may involve more than one physical mechanism.

5. ACKNOWLEDGEMENTS

The authors are grateful for the financial support from the PPGEM – UNESP/FEIS, from CAPES, from CNPq (grant number 458702/2014-5) and from FAPESP (grants numbers 2013/15431-7, 2014/19497-5 e 2016/02034-8).

6. REFERENCES

Cardoso, E.M., Kannengieser, O., Stutz, B., Passos, J.C., 2011. “FC72 and FC87 nucleate boiling inside a narrow horizontal space”, *Experimental Thermal and Fluid Science* 35, pp.1038–1045.

Cardoso, E.M., Passos, J.C., 2013. “Nucleate boiling of n-pentane in a horizontal confined Space”, *Heat Transfer Eng.* 34, pp. 470–478

Ishibashi, E. and Nishikawa, K., 1969. “Saturated boiling heat transfer in narrow spaces”. *International Journal of Heat and Mass Transfer*, Vol.12, pp. 863-866.

Katto, Y., Yokoya, S., Teraoka, K., 1977. “Nucleate and transition boiling in a narrow space between two horizontal parallel disk-surface”. *Bull. JSME* 20 (143), pp. 638–643.

Kiyomura, I.S.; Manetti, L.L.; Da Cunha, A.P.; Ribatski, G. and Cardoso, E.M., 2017. “An analysis of the effects of nanoparticles deposition on characteristics of the heating surface and on pool boiling of water”. *International Journal of Heat and Mass Transfer*, vol. 106, p. 666.

Nunes, J. M., Manetti, L. L., Cardoso, E. M., 2017. “Experimental analysis of nucleate boiling on nanostructured surfaces under confined conditions”. In *Proceedings of the 24th ABCM International Congress of Mechanical Engineering COBEM2017*. Curitiba, Brazil.

Passos, J.C., Hirata, F.R., Possamai, L.F.B., Balsamo, M., Misale, M., 2004. “Confined boiling of FC72 and FC87 on a downward facing heating copper disk”, *International Journal of Heat Fluid Flow 25* (2), pp.313–319.

Souza, R.R., Passos, J.C., Cardoso, E.M., 2014. “Influence of nanoparticle size and gap size on nucleate boiling using HFE7100”. *Experimental Thermal and Fluid Science*, Vol.59, pp. 195- 201.

Souza, R.R., Passos, J.C., Cardoso, E.M., 2018. “Confined and unconfined nucleate boiling of HFE7100 in the presence of nanostructured surfaces”. *Experimental Thermal and Fluid Science*, Vol.91, pp. 312-319.

Takata, Y., Hidaka, S., Cao, J.M., Nakamura, T., Yamamoto, H., Masuda, M. and Ito, T., 2005. “Effect of surface wettability on boiling and evaporation.” *Energy* Vol. 30, pp. 209-220.

Yang, C.Y. and Liu, C.F., 2013. “Effect of coating layer thickness for boiling heat transfer on micro porous coated surface in confined and unconfined spaces”. *Experimental Thermal and Fluid Science*, Vol. 47, pp. 40-47.

Yao, S. C. and Chang, Y., 1983. “Pool boiling heat transfer in a confined space”. *International Journal of Heat and Mass Transfer*, Vol. 26, p. 841-848.

7. RESPONSIBILITY NOTICE

The authors are the only responsible for the printed material included in this paper.